Journal of Alloys and Compounds 488 (2009) 279–283

Contents lists available at ScienceDirect

Journal of Alloys and Compounds

journal homepage: www.elsevier.com/locate/jallcom

The structure and mechanical properties of as-cast Zr–Ti alloys

Hsueh-Chuan Hsu[a,b], Shih-Ching Wu[a,b], Yu-Chih Sung[c], Wen-Fu Ho[d,*]

[a] Department of Dental Laboratory Technology, Central Taiwan University of Science and Technology, Taichung, Taiwan, ROC
[b] Institute of Biomedical Engineering and Material Science, Central Taiwan University of Science and Technology, Taichung, Taiwan, ROC
[c] Department of Mechanical and Automation Engineering, Da-Yeh University, Changhua, Taiwan, ROC
[d] Department of Materials Science and Engineering, Da-Yeh University, No. 168, University Road, Dacun, Changhua 515, Taiwan, ROC

ARTICLE INFO

Article history:
Received 30 July 2009
Accepted 22 August 2009
Available online 27 August 2009

Keywords:
Metals and alloys
X-ray diffraction
Microstructure
Mechanical properties

ABSTRACT

This study has investigated the structure and mechanical properties of pure Zr and a series of binary Zr–Ti alloys in order to determine their potential application as dental implant materials. The titanium contents of these alloys range from 10 to 40 wt.% and were prepared by arc melting in inert gas. This study evaluated the phase and structure of these Zr–Ti alloys using an X-ray diffraction (XRD) for phase analysis, and an optical microscope for microstructure analysis of the etched alloys. Three-point bending tests were performed to evaluate the mechanical properties of all specimens. The experimental results indicated that the pure Zr and Zr–10Ti comprised entirely of an acicular hexagonal structure of α′ phase. When the Ti content increased to 20 wt.%, a significant amount of β phase was retained. However, when the Ti content increased to 40 wt.%, only the equi-axed, retained β phase was observed in the cast alloy. Moreover, the hardness values and bending strengths of the Zr–Ti alloys decreased with an increasing Ti content. Among pure Zr and Zr–Ti alloys, the α′-phase Zr–10Ti alloy has the greatest hardness and bending strength. The pure Zr and Zr–Ti alloys exhibit a similar elastic modulus ranging from 68 GPa (Zr–30Ti) to 78 GPa (Zr–40Ti). Based on the results of elastic moduli, pure Zr and Zr–Ti alloys are found to be suitable for implant materials due to lower modulus. Like bending strength, the elastically recoverable angle of Zr–Ti alloys decreased as the concentration of Ti increased. In the current search for a better implant material, the Zr–10Ti alloy exhibited the highest bending strength/modulus ratios as large as 25.3, which are higher than that of pure Zr (14.9) by 70%, and commercially pure Ti (8.7) by 191%. Thus, Zr–Ti alloy's low modulus, ductile property, excellent elastic recovery capability and impressive strength confirm that it is a promising candidate for dental implant materials.

1. Introduction

Ti and some of its alloys are preferred load-bearing implant materials due to their relatively low modulus, excellent strength-to-weight ratio, good fracture toughness, and superior biocompatibility and corrosion resistance [1]. The use of titanium and its alloys in orthopedic applications has mainly been limited to the alloy Ti–6Al–4 V and to commercially pure titanium (c.p. Ti). Although these materials were initially used for military and aircraft construction, the medical application of both c.p. Ti and Ti–6Al–4 V have also been used since the 1960s. Ti–6Al–4 V gradually replaced c.p. Ti because comparably, the former has a greater mechanical strength in application to plates, nails, screws and endo-prostheses [2]. However, speculation that the release of Al and V ions from the alloy might cause some long-term health problems [3–5] has prompted additional studies that explore the potential for alternative implant materials.

Zr alloys have been used as structural materials in nuclear and chemical engineering applications for many years. There are recent publications addressing the use of Zr and other refractory metals systems for bio-implants [6–9]. Zr offers superior corrosion resistance over most other alloy systems across a wide range of environments [10]. Additionally, Zr metal shows acceptable mechanical strength and satisfactory biocompatibility [11–13]; thereby it is a material of interest for surgical implants [14–18]. In vivo evidence has indicated that zirconium implants exhibit good osseointegration [19,20] and studies comparing zirconium and titanium implants showed that the degree of bone-implant contact is actually higher in the case of zirconium [21].

Both zirconium and titanium belong to the same group in the periodic table of elements, and are known to have similar chemical properties. In addition, they are also reported to have good corrosion resistance and biocompatibility [12,13,22,23]. Since the Ti–Zr system shows as a complete solid solution for both the high

* Corresponding author. Tel.: +886 4 8511888x4108; fax: +886 4 8511224.
E-mail address: fujii@mail.dyu.edu.tw (W.-F. Ho).

0925-8388/$ – see front matter © 2009 Elsevier B.V. All rights reserved.
doi:10.1016/j.jallcom.2009.08.105

temperature beta phase and the low temperature alpha phase [24], a wide variation of alloy design is available. In our previous studies, the structure and mechanical properties of a series of binary Ti–Zr alloys with Zr contents up to 40 wt.% had been investigated [25]. In addition to these studies, the mechanical properties and grindability of a binary Ti–Zr alloy when added to a series of alloying elements (Nb, Mo, Cr and Fe) was also evaluated [26]. In our present study, we investigate the structure and mechanical properties by conducting bending tests for a series of binary Zr–Ti alloys with Ti contents up to 40 wt.%. There is a particular emphasis on further improvement in the strength/modulus ratio as this may be an indication of feasibility for use as implant material [27].

2. Materials and methods

The materials used for this study include pure Zr, Zr–10Ti, Zr–20Ti, Zr–30Ti and Zr–40Ti alloys (in wt.%). All the materials have been prepared from raw titanium (99.8% in purity), and Zr (99.95% in purity) using a commercial arc-melting vacuum-pressure-type casting system (Castmatic, Iwatani Corp., Japan). The melting chamber was first evacuated and purged with argon, then maintained using a pressure of 1.5 kg f/cm^2 during the melting process. Appropriate amounts of metals were melted in a U-shaped copper hearth with a tungsten electrode. The ingots were re-melted five times prior to casting to improve chemical homogeneity. Prior to casting, the ingots were melted once again in an open-based copper hearth under an argon pressure of 1.5 kg f/cm^2. The difference in pressure between the two chambers allowed the molten alloys to instantly drop into the graphite mold.

The cast alloys were sectioned using a Buehler Isomet low-speed diamond saw to obtain specimens for various purposes. Surfaces of the alloys for microstructural study were mechanically polished via a standard metallographic procedure to a final level of 0.3 μm alumina powder and then etched in a solution of water, nitric acid, and hydrofluoric acid (80:15:5 in volume). Microstructure of the etched alloys was examined using an optical microscope (BH2, Olympus, Japan). X-ray diffraction (XRD) for phase analysis was conducted using a diffractometer (XRD-6000, Shimadzu, Japan) operated at 30 kV and 30 mA. Ni-filtered CuKα radiation was used for this study. Phase was identified by matching each characteristic peak with the JCPDS files. The microhardness of polished alloys was measured using a microhardness tester (MVK-E3, Mitutoyo, Japan) at 100 g for 15 s.

Three-point bending tests were performed using a desk-top mechanical tester (AG-IS, Shimadzu, Japan). The bending strengths were determined using the equation, $\sigma = 3PL/2bh^2$ [28], where σ is the bending strength (MPa), P the load (N), L the span length (mm), b the specimen width (mm), and h the specimen thickness (mm). The span length was $L = 30$ mm, and the dimensions of the specimens were $b = 5.0$ mm and $h = 1.0$ mm. The modulus of elasticity in bending is calculated from the load increment and the corresponding deflection increment between the two points on the straight line as far apart as possible using the equation $E = L^3\Delta P/4bh^3\Delta\delta$. In this representation, E is the modulus of elasticity in bending (Pa), ΔP the load increment as measured from the preload (N), and $\Delta\delta$ the deflection increment at mid-span as measured from the preload. The average bending strength and modulus of elasticity in bending were taken from at least five tests under each condition. The elastic recovery (spring-back) capability for each material was evaluated from the change in deflection angle when loading was removed. Details can be found in Ho et al. [29].

3. Results and discussion

3.1. X-ray diffraction

The XRD patterns of cast pure Zr and the series of binary Zr–Ti alloys are shown in Fig. 1. The XRD results indicated that crystal structure of the as-cast Zr–Ti alloy is sensitive to the composition (Ti content) of the alloy. As shown in Fig. 1, the pure Zr and Zr–10Ti comprised entirely of a hexagonal α′ phase. When the Ti content increased to 20 wt.%, a significant amount of β phase was retained. When the Ti content increased to 40 wt.%, only the retained β phase was observed in the cast alloy.

Zirconium and titanium belong to the IVB group in the periodic table and are known to have similar structure and chemical properties. A martensitic allotropic transformation exists between the low temperature α phase (hexagonal close packed) and the high temperature β phase (body centered cubic), which is stable until the melting occurs. The binary phase diagram presents a continuous solid solution between α and β phases [24]. By comparison, due to the smaller atomic radius of Ti (1.47 Å) than Zr (1.62 Å), the addition of Ti caused the α′ and β phase lattice parameters to decrease, which in turn caused the XRD peaks to shift toward high angle side. The higher the Ti content, the more obvious the shift, as shown in the XRD patterns.

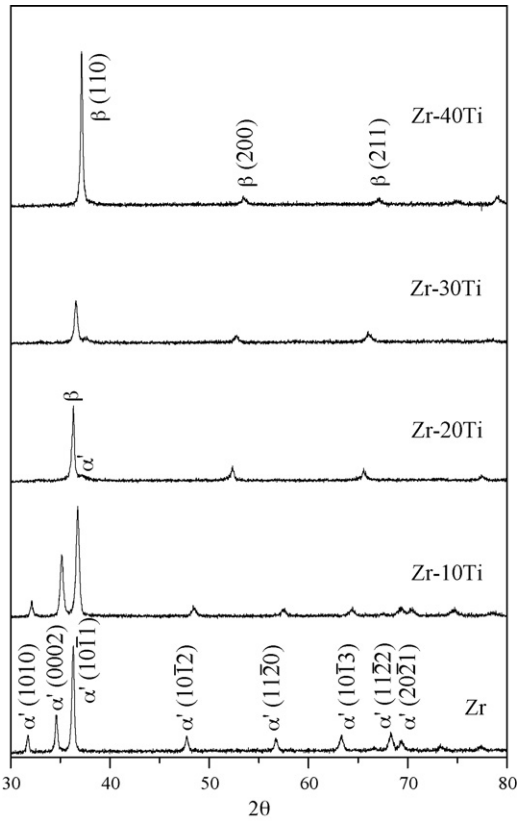

Fig. 1. X-ray diffraction patterns of pure Zr and Zr–Ti alloys.

3.2. Light microscopy

The microstructure of pure Zr and the series of Zr–Ti alloys, as shown in Fig. 2, were in agreement with the XRD results. The pure Zr exhibited a fine, acicular martensite microstructure, and the Zr–10Ti alloy also exhibited acicular structure of α′ phase. When the Ti content increased to 20 wt.%, a significant amount of equiaxed, retained β phase was observed and co-existed with α′ phase. When the alloy contained 40 wt.% Ti, β phase became the only dominant phase. Apparently, when Ti was added, the martensitic start (Ms) temperature became lower than room temperature and the martensitic transformation was suppressed [30]. In other words, in the Zr–Ti alloy system, β phase could be entirely retained upon fast cooling when the Zr content was higher than approximately 40 wt.%, proving its consistency with the XRD results.

3.3. Mechanical properties

The microhardness values of pure Ze and Zr–Ti alloys are shown in Fig. 3. The hardness of pure Zr was 175 HV, whereas the hardness of the Zr–Ti alloys became slightly lower as the Ti was added, and ranged from 275 HV (Zr–30Ti) to 291 HV (Zr–10Ti). All the Zr–Ti alloys had significantly higher ($p < 0.05$) hardness than the pure Zr tested. The hardness of Zr–10Ti alloy with α′ phase were significantly higher ($p < 0.05$) than that of Zr–40Ti alloy containing only β phase. Additionally, Lee et al. [31] also reported that the β phase alloy has the lowest hardness level in Ti–Nb system.

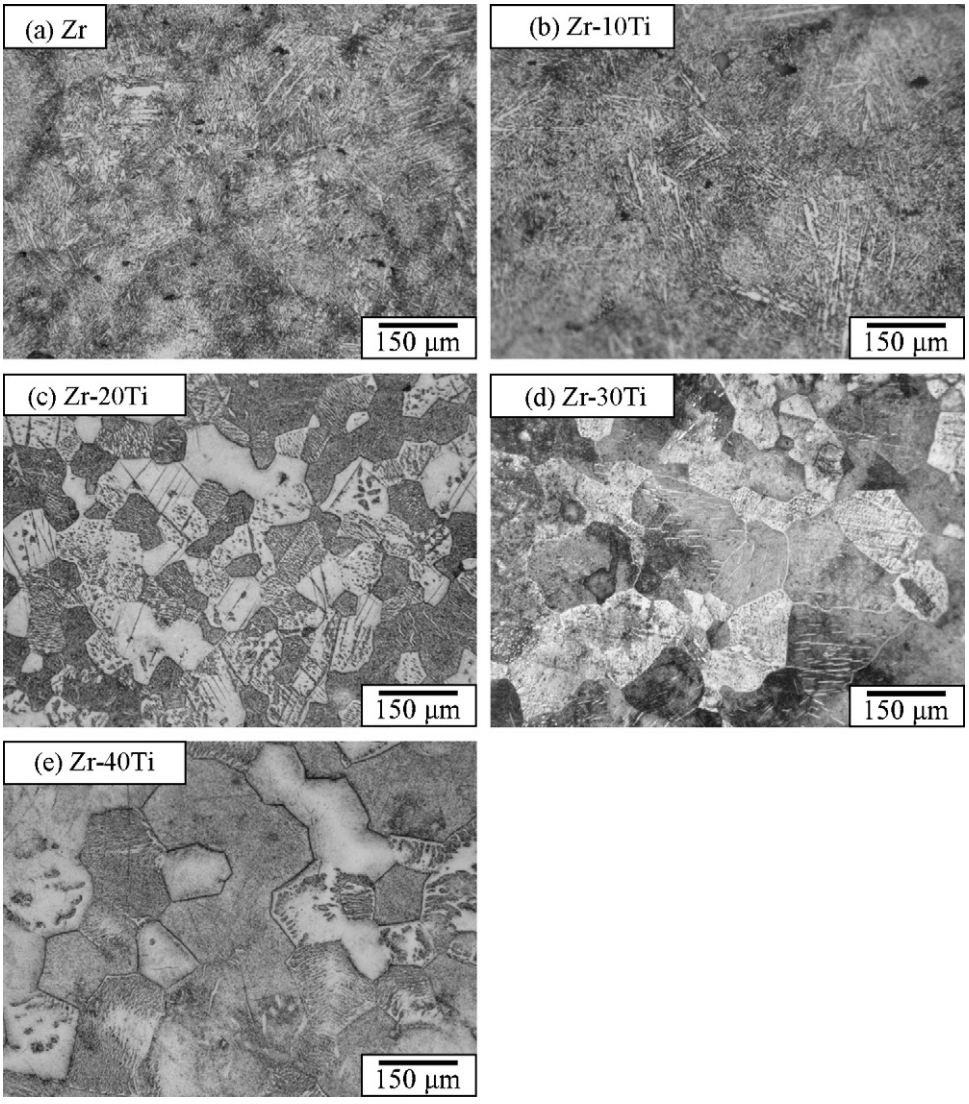

Fig. 2. Light micrographs of pure Zr and Zr–Ti alloys.

Consistent with the microhardness values, the bending strengths of all the Zr–Ti alloys (1258–1738 MPa) were significantly higher ($p < 0.05$) than that of pure Zr (1142 MPa), as shown in Fig. 4. The bending strengths of the Zr–Ti alloys decreased with an increasing Ti content. The bending strength of Zr–40Ti alloy was slightly higher than that of Zr–30Ti probably due to a solid solution-strengthening effect, although there were no significant differences ($p > 0.05$) between Zr–30Ti and Zr–40Ti. It is worth noting that α′-

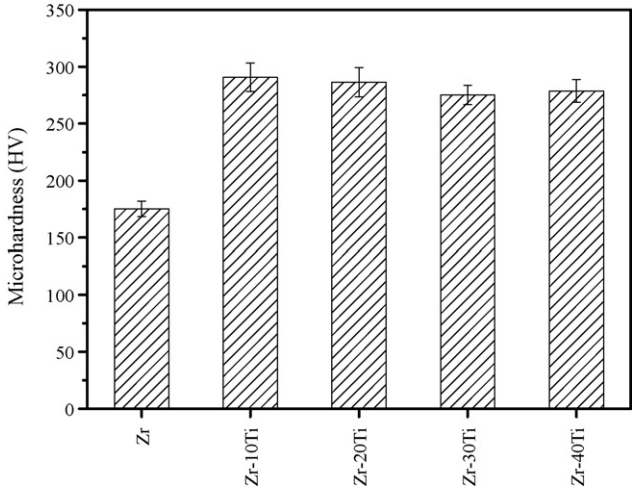

Fig. 3. Micro-hardness of pure Zr and Zr–Ti alloys.

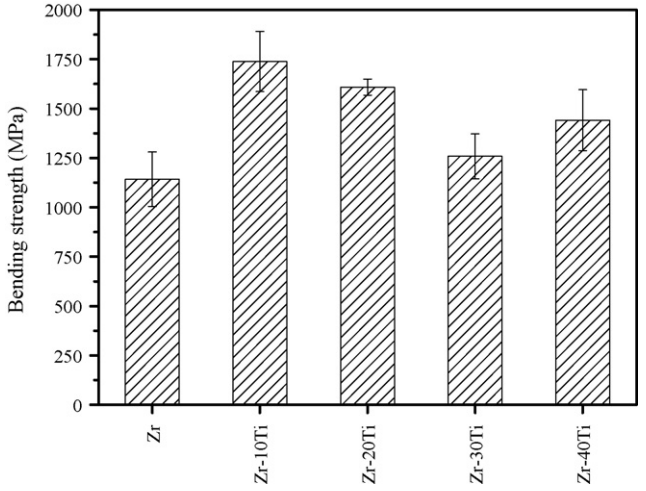

Fig. 4. Bending strengths of pure Zr and Zr–Ti alloys.

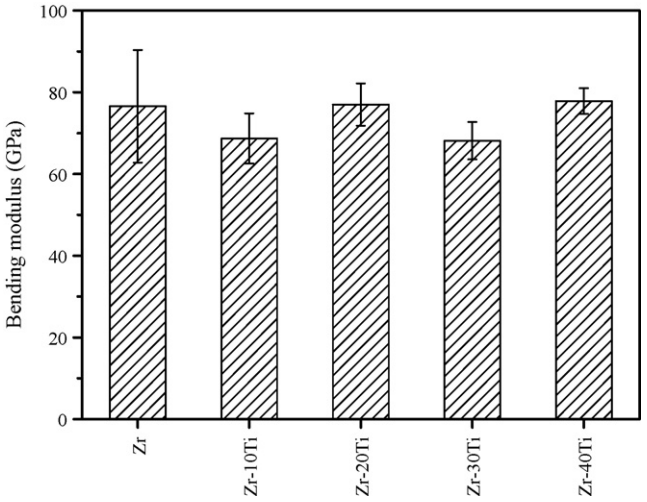

Fig. 5. Bending moduli of pure Zr and Zr–Ti alloys.

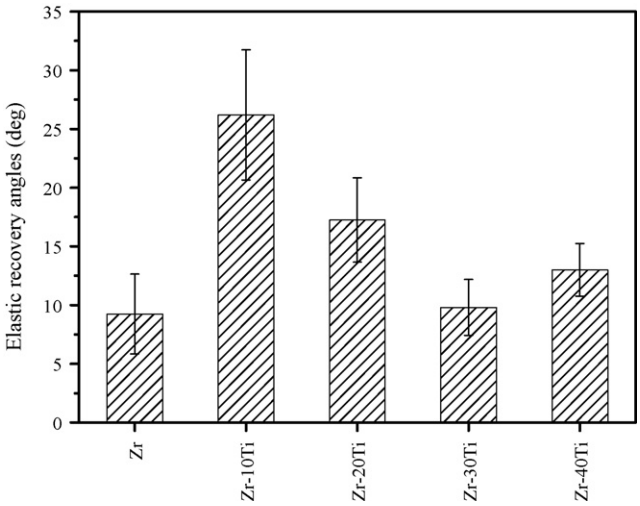

Fig. 7. Elastic recovery angles of pure Zr and Zr–Ti alloys.

phase Zr–10Ti alloy had the greatest bending strength among pure Zr and Zr–Ti alloys. A similar result was observed in the Ti–Nb system by Lee et al. [31], who proposed that the α′ phase-dominated alloy had a higher bending strength, while the β phase alloy had a lower strength.

The elastic modulus results are shown in Fig. 5. The pure Zr and Zr–Ti alloys exhibit similar elastic modulus ranging from 68 GPa (Zr–30Ti) to 78 GPa (Zr–40Ti). Of the Zr–Ti alloys, the alloy with 30 wt.% Ti content shows the lowest bending modulus, and it had a significantly lower ($p < 0.05$) bending modulus than Zr–20Ti and Zr–40Ti alloys. However, amongst the Zr–Ti alloys, there were no significant differences from the pure Zr with regard to bending modulus ($p > 0.05$). Moreover, it is worth noting that the bending moduli of pure Zr and Zr–Ti alloys are significantly lower ($p < 0.05$) than that of c.p. Ti (99 GPa) [29]. Using implant materials with lower moduli (closer to that of human bone) could reduce the stress shielding effect [32,33] (i.e., insufficient loading of bone due to the large difference in modulus between the implant device and its surrounding bone). As a result, the relatively low moduli of pure Zr and Zr–Ti alloys seem to be promising candidates for implant materials.

The typical bending stress-deflection profiles of the series of alloys and pure Zr are shown in Fig. 6. All the Zr–Ti alloys and pure Zr did not fail, even after being deflected by 8 mm (the pre-set maximum). In addition, all the Zr–Ti alloys and pure Zr exhibited ductile properties. Fig. 7 shows the means of the elastic recovery capability of Zr–Ti alloys decreased as the concentration of Zr increased. This trend is similar to that in bending strength, and a similar result was also observed in the Ti–Zr system [25]. It is worth noting that the advantage in mechanical properties of the Zr–10Ti alloy is also demonstrated in their high elastic recovery capability. High elastic recovery (spring-back) capability of a metal is an indication of high strength and low modulus and is essential for many load-bearing implant and dental applications. The elastic recovery capability of the Zr–10Ti alloy was significantly greater ($p < 0.05$) than pure Zr and all the other Zr–Ti alloys fabricated in this study. For example, the elastically recoverable angle of the Zr–10Ti alloy (26.2°) was higher than that of pure Zr (9.5°) by as much as 176%. Moreover, it was even greater than that of c.p. Ti (2.7°) [25] by as much as 870%.

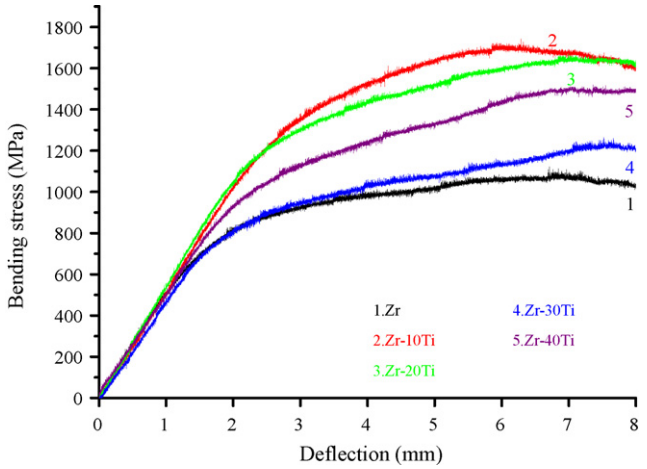

Fig. 6. Bending stress-deflection profiles of pure Zr and Zr–Ti alloys.

In the current search for a better implant material, the Zr–10Ti alloy proves to serve as a promising candidate. This study has determined that the alloy not only exhibits a low modulus, but also displays ductile property, excellent elastic recovery capability and impressive strength (or high strength/modulus ratio). This particular composition results in a bending strength/modulus ratio as large as 25.3, which is higher than that of pure Zr (14.9) and c.p. Ti (8.7) [34] by 70% and 191%, respectively.

4. Conclusions

The following conclusions can be drawn from this study:

(1) Based on the results of XRD and optical microscopy, the Zr–10Ti alloy showed hcp α' structures. With 20 wt.% Ti, metastable β phase starts to be retained. When the Ti content is increased to 40 wt.%, retained β phase became the only dominant phase.
(2) All the Zr–Ti alloys had significantly higher hardness than pure Zr tested. The hardness of Zr–10Ti alloy with α' phase was higher than that of Zr–40Ti alloy containing only β phase.
(3) The bending strengths of all the Zr–Ti alloys (1258–1738 MPa) were higher than that of pure Zr (1142 MPa). The bending strength of the Zr–10Ti alloy was greater than that of pure Zr by 52%.
(4) The pure Zr and Zr–Ti alloys exhibit similar elastic modulus ranging from 68 GPa (Zr–30Ti) to 78 GPa (Zr–40Ti). Those are significantly lower than that of c.p. Ti (99 GPa).
(5) The elastic recovery capability of Zr–10Ti alloy was significantly greater than pure Zr and all the other Zr–Ti alloys fabricated in this study. Furthermore, the Zr–10Ti alloy exhibited the highest

bending strength/modulus ratios as large as 25.3, higher than that of pure Zr (14.9) by 70%, and of c.p. Ti (8.7) by 191%.

References

[1] M. Long, H.J. Rack, Biomaterials 19 (1998) 1621–1639.
[2] E. Eisenbarth, D. Velten, M. Müller, R. Thull, J. Breme, Biomaterials 25 (2004) 5705–5713.
[3] P.R. Walker, J. LeBlanc, M. Sikorska, Biochemistry 28 (1989) 3911–3915.
[4] S. Yumoto, H. Ohashi, H. Nagai, S. Kakimi, Y. Ogawa, Y. Iwata, K. Ishii, Int. J. PIXE 2 (1992) 493–504.
[5] S. Rao, T. Ushida, T. Tateishi, Y. Okazaki, S. Asao, Biomed, Mater. Eng. 6 (2) (1996) 79–86.
[6] M.D. Ries, A. Salehi, K. Widding, G. Hunter, J. Bone Joint Surg. 84 (2002) 129–135.
[7] A.M. Patel, M. Spector, Biomaterials 18 (1997) 441–447.
[8] X.B. Chen, A. Nouri, P.D. Hodgson, C.E. Wen, Advan. Mater. Res. 15–17 (2007) 89–94.
[9] N.T.C. Oliveira, S.R. Biaggio, S. Piazza, C. Sunseri, F. Di Quarto, Electrochem. Acta 49 (2004) 4563–4576.
[10] N. Stojilovic, E.T. Bender, R.D. Ramsier, Prog. Surf. Sci. 78 (2005) 101–184.
[11] L. Saldana, A. Méndez-Vilas, L. Jiang, M. Multigner, J.L. González-Carrasco, M.T. Pérez-Prado, M.L. González-Martín, L. Munuera, N. Vilaboa, Biomaterials 28 (2007) 4343–4354.
[12] Y. Okazaki, S. Rao, T. Tateishi, Y. Ito, Mater. Sci. Eng. A 243 (1998) 250–256.
[13] M. Niinomi, Biomaterials 24 (2003) 2673–2683.
[14] P. Gehrke, G. Dhom, J. Brunner, D. Wolf, M. Degidi, A. Piattelli, Quintessence Int. 37 (2006) 19–26.
[15] K.M. Sherepo, A.B. Parfenov, I.S. Zusmanovich, Med. Tekh. 5 (1992) 14–16.
[16] M. Niinomi, J. Miner. Met. Mater. Soc. 51 (1999) 32–34.
[17] P. Thompsen, C. Larsson, L.E. Ericson, L. Sennerby, J. Lausmaa, B. Kasemo, J. Mater. Sci. Mater. Med. 8 (1997) 653–665.
[18] K.M. Sherepo, I.A. Red'ko, Med. Tekh. 2 (2004) 22–24.
[19] R.L. Cabrini, M.B. Guglielmotti, J.C. Almagro, Implant Dent. 2 (1993) 264–267.
[20] M.B. Guglielmotti, C. Guerrero, R.L. Cabrini, Acta Odontol. Latinoam. 10 (1997) 11–23.
[21] M.B. Guglielmotti, S. Renou, R.L. Cabrini, Int. J. Oral Maxillofac. Implants 14 (1999) 565–570.
[22] Y. Okazaki, S. Asao, S. Rao, T. Tateishi, J. Jpn. Inst. Met. 60 (1996) 902–906.
[23] D.L. Douglass, At. Energy Rev. 3 (1963) 71–237.
[24] J.L. Murray, in: J.L. Murray (Ed.), Phase Diagrams of Binary Titanium Alloys, ASM International, Materials Park, OH, 1987, p. 340.
[25] W.F. Ho, W.K. Chen, S.C. Wu, H.C. Hsu, J. Mater. Sci. Mater. Med. 19 (2008) 3179–3186.
[26] W.F. Ho, C.H. Cheng, C.H. Pan, S.C. Wu, H.C. Hsu, Mater. Sci. Eng. C 29 (2009) 36–43.
[27] C.M. Lee, W.F. Ho, C.P. Ju, J.H. Chern Lin, J. Mater. Sci. Mater. Med. 13 (2002) 695–700.
[28] A. Guha, in: H.E. Boyer, T.L. Gall (Eds.), Metals Handbook, vol. 8, ninth ed., ASM International, Materials Park, OH, 1985, pp. 133–136.
[29] W.F. Ho, C.P. Ju, J.H. Chern Lin, Biomaterials 20 (1999) 2115–2122.
[30] S. Kobayashi, K. Nakai, Y. Ohmori, Mater. Trans. 42 (2001) 2398–2405.
[31] C.M. Lee, C.P. Ju, J.H. Chern Lin, J. Oral Rehab. 29 (2002) 314–322.
[32] D.R. Sumner, J.O. Galante, Clin. Orthop. Relat. Res. 274 (1992) 202–212.
[33] E. Cheal, M. Spector, W. Hayes, J. Orthop. Res. 10 (1992) 405–422.
[34] W.F. Ho, T.Y. Chiang, S.C. Wu, H.C. Hsu, J. Alloys Compd. 468 (2009) 533–538.